Characterization of TiO$_2$ Nanoparticle's Morphology and its Influence on the Hydrogen Sorption Kinetics of MgH$_2$

Anderson de Farias Pereira[a]*[ID], Sidnei Paciornik[b], Dilson Silva dos Santos[a][ID], Paula Mendes Jardim[a]

[a]*Departamento de Engenharia Metalúrgica e de Materiais, Instituto Alberto Luiz Coimbra de Pós-Graduação e Pesquisa de Engenharia (COPPE), Universidade Federal do Rio de Janeiro (UFRJ), Rio de Janeiro, RJ, Brasil*
[b]*Departamento de Engenharia Química e de Materiais, Pontifícia Universidade Católica do Rio de Janeiro (PUC-Rio), Rio de Janeiro, RJ, Brasil*

TiO$_2$ nanorods present good performance as catalysts in the sorption behavior of magnesium hydride. In the present study, the morphology of TiO$_2$ nanorods produced from titanate nanotubes heat-treated at 550 °C (NR550), 650 °C (NR650) and 750 °C (NR750) was characterized and their catalytic role on the sorption kinetics of MgH$_2$ was evaluated. For this, ball-milled MgH$_2$-TiO$_2$ nanocomposites with 5 wt% of additives were prepared and the materials were characterized by X-ray diffraction (XRD), BET surface area and Transmission Electron Microscopy (TEM). The hydrogen sorption kinetics of the composites were evaluated in a Sievert's apparatus at 350 °C. The results indicated that NR550 and NR650 consisted of a mixture of nanorods and nanoparticles and NR750 of coarser nanoparticles of TiO$_2$-anatase with a small amount of rutile. Composites with NR750 and NR550 presented the best sorption kinetics, suggesting the positive effect of the presence of rutile and of anatase nanorods, respectively, on the sorption properties of the material.

Keywords: *hydrogen storage, magnesium hydride, TiO$_2$ nanorods, 1D nanomaterials.*

1. Introduction

Even before the genesis of the Hydrogen Economy concept, metal hydrides have been used in a wide range of industrial applications: from additives in steelmaking processes and reagents in the chemical industry to neutron shielding materials in nuclear reactors[1,2]. However, a new highlight was given to these materials as hydrogen started to be increasingly more considered as a potential candidate for a cleaner and more versatile substitute to fossil fuels[3,4]. This trend can be indicated by the growing market of hydrogen storage materials and technologies, which responded to about 3.6 billion dollars in 2016, according to a report by BCC Research[5].

The reason for the use of these materials in hydrogen storage applications relies on their high volumetric capacity and their ability to absorb and desorb hydrogen with a small variation in pressure. Among them, MgH$_2$ is found to be interesting due to its high gravimetric capacity (about 7.6 wt%) and low density (1.7 g/cm³), making it a promisor candidate for lightweight applications. However, despite its good gravimetric storage capacity, the need for moderate to high temperatures (around 300-400 °C) for hydrogen desorption and the slow transformation kinetics of the system Mg-MgH$_2$ are the main challenges for their use. The high working temperatures are related to the thermodynamic stability of the MgH$_2$ compound while the slow absorption/desorption kinetics are attributed to either the passivation of magnesium surfaces (by rapid oxide/hydroxide layer formation), the low hydrogen diffusivity in magnesium hydride (D_H=5.8 x 10^{-14} cm²/s at 20 °C)[6–8] or the slow dissociation/recombination kinetics of hydrogen molecules over magnesium surface[9,10].

In this sense, many studies have been done with the intent of increasing the sorption kinetics of Mg/MgH$_2$ by the addition of catalysts. One of the strategies adopted is the addition of transition metal oxide catalysts by the production of nanocomposites with MgH$_2$ by means of high energy ball milling. Among them, TiO$_2$ is shown to be an interesting candidate due to the good catalytic performance associated with its low cost and high availability. Besides the composition, many studies indicate that the nanoparticle's morphology is an important parameter when considering catalytic performance in many systems[11–16]. With respect to hydrides, various studies point out that the 1D morphology of catalysts might have a beneficial effect on the sorption kinetics of hydrides systems[17–19], and specifically, positive results have been observed for TiO$_2$-based nanomaterials with 1D morphology added to MgH$_2$[20,21].

In such a manner, the goal of this study can be divided into two aspects: (i) the morphology characterization through TEM of 1D TiO$_2$ nanoparticles – produced through three different heat treatment routes from titanate nanotubes – and (ii) their effect on the hydrogen sorption kinetics in nanocomposites of MgH$_2$-TiO$_2$ produced by high energy ball milling.

2. Experimental Procedures

2.1 Sample preparation

The production of the catalysts used in this study started with the synthesis of hydrogen titanate nanotubes via an

*e-mail: afpereira@metalmat.ufrj.br

alkaline hydrothermal route described by Kasuga *et al.*[22], followed by a subsequent heat treatment at 550 °C, 650 °C and 750 °C for 2 h (named NR550, NR650 and NR750, respectively) in order to produce TiO_2-anatase nanorods (which are observed to form for heat treatment at 550°C/2h[23]). The heat treatment temperatures were chosen in order to evaluate the evolution in size and morphology of the TiO_2 nanomaterials with temperature increase.

For the preparation of the MgH_2-TiO_2 nanocomposites, commercial MgH_2 powder (Sigma Aldrich, 99.4%) was submitted to a two-step ball-milling process consisting of a 24 h milling of pure MgH_2 followed by a 20 minutes milling after addition of 5 wt% of catalyst, both at 300 RPM. The ball milling was carried out under 2 bar of H_2 atmosphere in a stainless steel crucible with tungsten carbide balls (8 balls of 20 mm in diameter) using a Fritsch P6 planetary mill. The samples were handled in a glove-box under argon atmosphere.

2.2 Sample characterization

Both the pure additives and the composites were analyzed by means of X-ray diffraction for phase identification and Transmission Electron Microscopy (TEM) was used for evaluation of morphology and dimensions of the catalysts as well as the distribution of catalysts within the MgH_2-TiO_2 composites. The XRD experiments were carried out in a Bruker D8 Discover powder diffractometer with Cu-κα radiation (40 kV, 40 mA) using a step size of 0.02° and step time of 0.6 s. The BET specific surface area of the nanomaterials used as catalysts in this study was determined using an Asap2020 Micromeritics instrument.

TEM images were obtained in an S/TEM Tecnai G20 FEG 200 kV and consisted of acquisitions of bright and dark-field images. A measure of the distribution of the particle's size and aspect ratio was obtained through the analysis of dark-field TEM images – acquired by the selection of a region of 101 diffraction ring of TiO_2-anatase with the objective aperture (centered dark-field) and by integration of the entire ring in a hollow-cone dark-field mode, as described in[24,25] – by means of a semi automatized image processing routine using *"Fiji-ImageJ v.1.52c"*[26]. The use of dark-field images was preferred for image processing for their simplest contrast information compared to the bright field ones and for the possibility of observing individual particles with no or low superposition effect.

The hydrogen sorption properties were investigated by kinetics tests in an automatic Sievert's type apparatus designed by PCT-Pro 8. The hydrogen absorption and desorption measurements were performed at 10 bar and 0.1 bar of hydrogen pressure, respectively, at 350 ºC. The kinetics curves were normalized to the maximum hydrogen capacity for each sample to give a better understanding of the evolution of fraction reacted with time.

2.3 Image processing routine

The image processing routine used was implemented in *"Fiji-ImageJ v.1.52c"*[26] and can be divided in two main steps: (i) processing of dark-field images (consisted of 4 steps: noise reduction by application of non-local means denoising filter[27], binarization through threshold, binary processing and identification of ROIs) and (ii) validation of the objects through comparison with bright field images followed by the evaluation of dimensions and shape of the objects. The parameters used for evaluating the particle's dimensions were the Feret's diameter and Min Feret's diameter, which corresponded to the particle's length and width, respectively, and, as a shape descriptor, the Aspect Ratio of the objects was considered.

3. Results and Discussion

3.1 Catalyst characterization

3.1.1 X-Ray diffraction

XRD of the samples NR550, NR650 and NR750 are shown in Figure 1. The analyses of the diffractogram show that the aforementioned samples are crystalline and composed mainly of TiO_2-anatase, which is in agreement with the expected for titanate nanotubes treated at 550 °C[11,23]. Some small intensity peaks related to TiO_2-rutile are observed for all samples, indicating a small content of this phase within the material, which increases for higher heat treatment temperatures. It is also interesting to highlight the narrowing of peak width as heat treatment temperature is increased, indicating that sample NR750 presents larger crystallites than NR650 while NR550 shows the smallest crystallite size of all the catalysts studied.
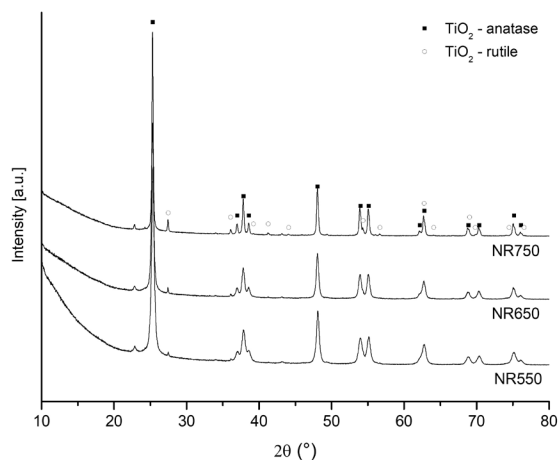
Figure 1. XRD patterns of samples NR550, NR650 and NR750.

3.1.2 Transmission Electron Microscopy

The TEM analyses of the catalysts studied showed that samples NR550 and NR650 consists of a mixture of nanorods and nanoparticles of TiO_2 anatase, with average size of 35.5 and 34.6 nm, respectively, while the sample treated at 750 °C (NR750) consists of nanoparticles of TiO_2 with coarser average size of about 69.4 nm as shown in Figure 2 and Table 2.
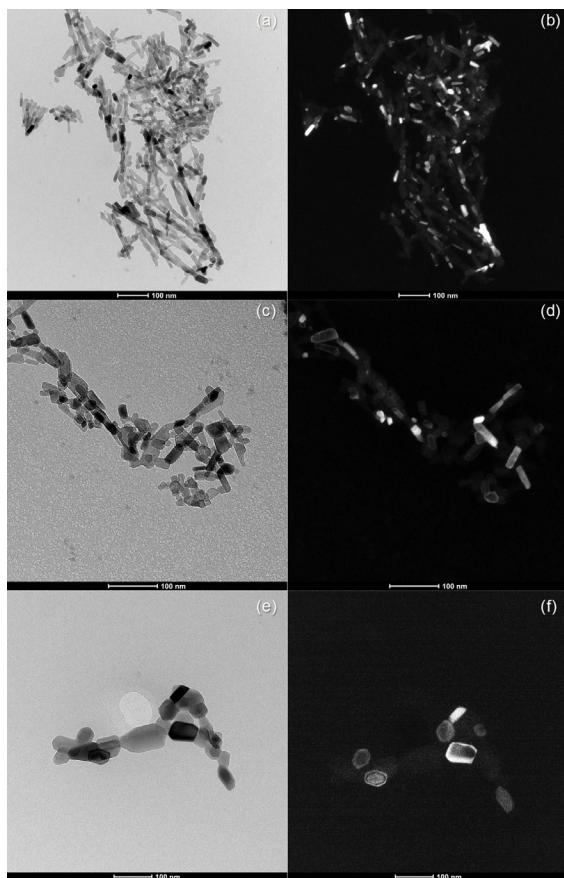
Figure 2. Bright-field (left) and Hollow-cone Dark-field (right) TEM images of the samples NR550 (a, b), NR650 (c, d) and NR750 (e, f).

It is also interesting to point out that the sample NR750 showed signs of sintering of nanoparticles (as highlighted in Figure 3).

The results of the quantitative analysis of TEM images of NR550, NR650 and NR750 are presented in the histograms and cumulative distributions of particle's length, width and aspect ratio presented in Figure 4 and summarized in Table 1.

It is important to point out that the obtained standard deviations were significantly high, especially for length measurements. This can be attributed to intrinsic errors from the dark-field image acquisition process (overlapping of diffracting nanoparticles or the formation of thickness fringes, for example), which introduce artifacts that can

Table 2. BET specific area for the samples NR550, NR650 and NR750.

Sample	BET Specific Area(m²/g)
NR 550	80,98
NR 650	57,61
NR 750	20,50

hinder the step of identification of ROIs after binarization. Nonetheless, it is observed that the distribution of particle's length and width were very similar for the samples NR550 and NR650, which presented practically the same average size. In contrast, the respective curves for the sample treated at 750 °C (NR750) were clearly shifted to greater values of particle size compared to the former ones.

With respect to the aspect ratio, it is possible to observe indications of a bimodal distribution (Figure 4 (e,f)) for the samples NR550 and NR650, pointing out the presence of nanoparticles and nanorods, and a trend of decrease in aspect ratio as heat treatment temperature increases, as indicated by Figure 4 (f), where it is observed that, considering an aspect ratio of 2 for comparison, sample NR550 presented 55% of particles with aspect ratio greater than 2, in contrast to 35% for NR650 and 8% for NR750.

3.1.3 Specific surface area

The specific BET surface area for the additives is presented in Table 2. This analysis shows that NR550 has the highest specific surface area among all the additives produced, with 81 m²/g followed by NR650 and NR750, which agree with the overall trend observed in XRD and TEM results. The higher decrease in specific surface area observed for the sample treated at 750 °C can be attributed not only to the coarsening of the nanoparticles, but also to the loss of their 1D character (which shows greater surface/volume ratio than 0D nanoparticles) and to the occurrence of sintering of nanoparticles as observed in TEM analysis.

3.2 Composite characterization

The XRD patterns of the samples after milling are shown in Figure 5 and indicated that all the samples presented similar constitution characterized by a mixture of MgH$_2$-β and MgH$_2$-γ (high-pressure metastable phase of magnesium hydride formed during milling[28]). Some peaks

Table 1. Average particle size and aspect ratio for the samples NR550, NR650 and NR750.

| Feature | Sample | | |
| | NR550 | NR650 | NR750 |
	Mean ± Standard Deviation	Mean ± Standard Deviation	Mean ± Standard Deviation
Length (Feret's Diameter)	35.47 ± 19.66 nm	34.62 ± 17.26 nm	69.42 ± 26.15 nm
Width (Min Feret's diameter) Aspect Ratio	14.11 ± 4.86 nm 2.70 ± 1.70	17.23 ± 5.83 nm 2.01 ± 0.96	45.15 ± 15.80 nm 1.50 ± 0.42
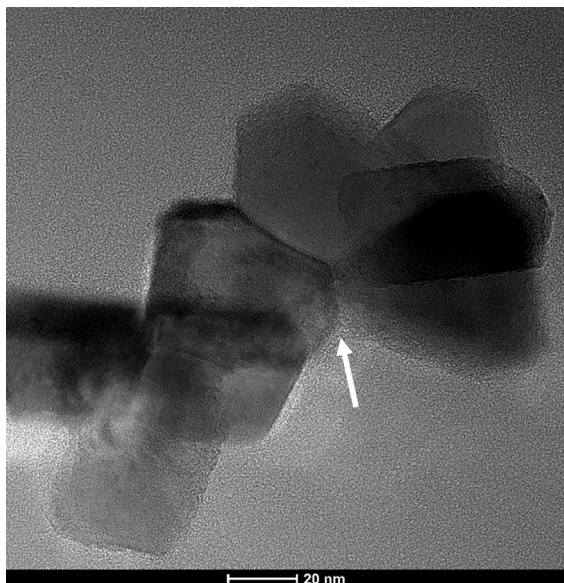
Figure 3. High-Resolution TEM image of NR750 showing grain boundary formation, indicating the occurrence of sintering of TiO_2 nanoparticles.

corresponding to metallic magnesium were also observed. It is important to highlight that no reflection corresponding to TiO_2 is observed in the composites samples (which can be related to the small content of catalysts added to MgH_2) and the absence of peaks corresponding to MgO or $Mg(OH)_2$ indicates that there was no oxidation of the samples during the preparation of the composites.

Although it was not possible to obtain a more detailed TEM evaluation of the composite after milling – due to the fast degradation of MgH_2 under the electron beam[21,29,30] and the small amount of thin agglomerates for a quantitative approach – a qualitative analysis of the MgH_2-TiO_2 composites indicated that the TiO_2 nanoparticles were fairly distributed within the composite matrix after milling, as shown in Figure 6.

3.2.1 Hydrogen sorption kinetics

The hydrogen sorption kinetics analyses of the composites showed that the addition of TiO_2 nanoparticles was beneficial to increase the kinetics in all the cases compared to the hydride before and after 24 h milling, as shown in the normalized hydrogen absorption and desorption curves presented in Figure 7.

During absorption, the composites with addition of NR750 and NR550 presented similar performance and their kinetics were superior to the observed for the sample with NR650. These results are consistent with the observed in previous works for TiO_2 anatase nanorods[21] and to the observed by GATTIA *et al.*[31] for pellets of MgH_2-TiO_2 composites containing 5 wt% of TiO_2 tested at 340°C/8bar, which absorbed about 50% of the maximum capacity after 5 minutes compared to 72% for the samples with NR750 and NR550 in the present study.

For desorption at 350 °C, the performance of the catalysts was significant, all of them having desorbed about 90% to 100% under 3 minutes, and were comparable to what was observed for composites of MgH_2 with TiO_2 nanorods and titanate nanotubes by JARDIM *et al.*[21].
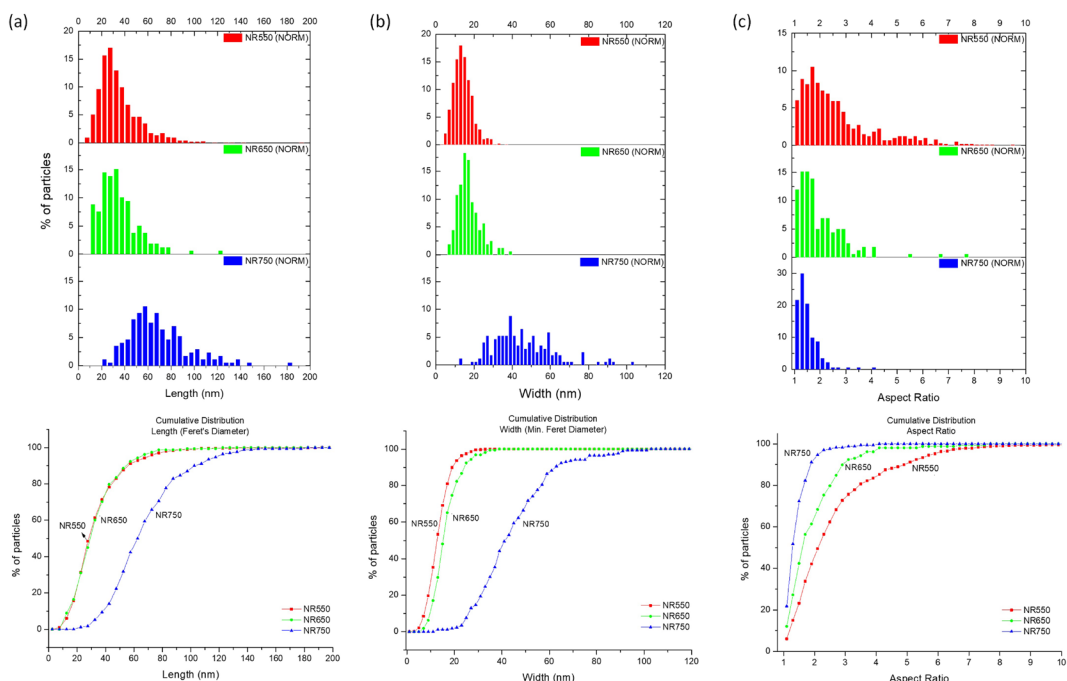
Figure 4. Comparative Histogram (top) and cumulative distribution (bottom) of particle's length (a), width (b) and aspect ratio (c) obtained from TEM analysis of samples NR550, NR650 and NR750.
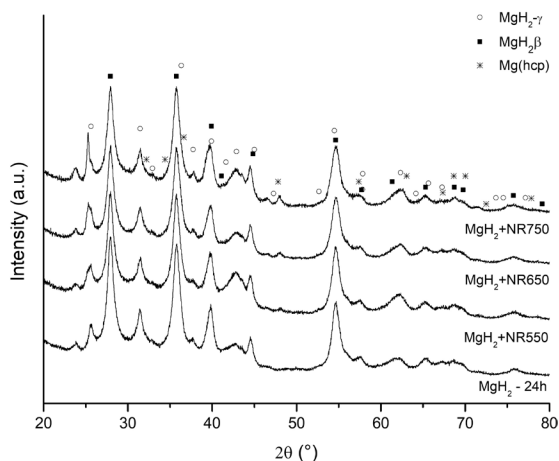
Figure 5. XRD patterns of pure MgH₂ after milling for 24 h and of composites of MgH₂ + 5 wt% of NR750, NR650 and NR550.
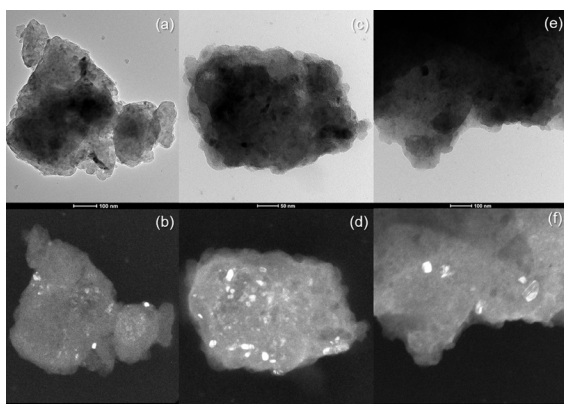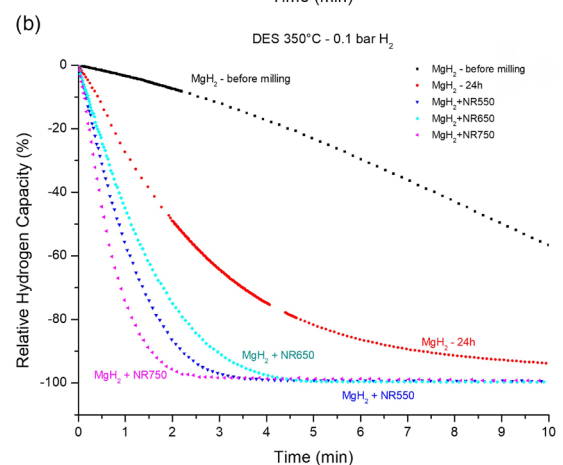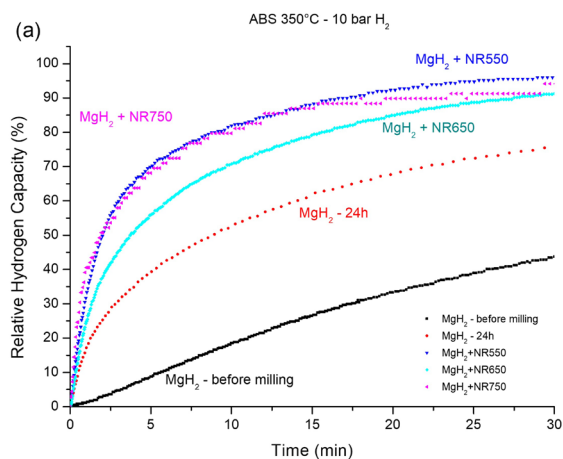

Figure 6. Bright field (top) and Centered Dark-Field (bottom) obtained for regions of (101) TiO₂-anatase diffraction ring for the samples MgH₂+NR550(a,b), MgH₂+NR650(c,d) and MgH₂+NR750(e,f), highlighting TiO₂ nanoparticles distributed within the hydride matrix.

Figure 7. Normalized hydrogen absorption (a) and desorption (b) kinetic curves at 350 ºC for samples of MgH₂ before and after 24 h milling at 300 rpm and of composites MgH₂+5wt% NR550, NR650 and NR750.

Comparing to other 1D materials, the kinetic performance of NR750 and NR550 were slightly faster than the observed for 1D niobates[17] in absorption and desorption at 350 °C and presented similar behavior in desorption compared to MWCNTs[19], also at 350 °C. For both cases, the composite preparation route used was similar to the one adopted in the present study.

Other works also investigated the results of addition of TiO₂ nanomaterials to MgH₂.[32–35] However, in reason of the differences in characterization techniques used and in the processing parameters (such as test temperature and pressure and milling energy and time), a direct comparison cannot be done.

Although there are differences between the TiO₂ nanomaterials studied in terms of their specific surface area, a direct correlation between the surface area and the performance of the catalysts in the hydrogen absorption or desorption from magnesium hydride was not observed.

The kinetics test showed that the catalyst with higher (NR550) and lower (NR750) specific areas showed similar results at absorption and the latter one performed better than the highest area catalyst in desorption at 350 °C.

The superior performance of the composite with NR750 might be attributed to the greater content of TiO₂-rutile present in this material compared to the other catalysts studied. This polymorph, as observed by JUNG *et al.*[36], PANDEY *et al.*[37] and VUJASIN *et al.*[38], tends to present better catalytic performance than TiO₂-anatase in hydrogen desorption from magnesium hydride. According to JUNG *et al.*[36], the better performance of rutile is attributed to the similarity in crystal structure (both being tetragonal of rutile type) and in cell parameters between TiO₂-rutile and MgH₂-β (a=b= 4.5163 Å and c = 3.0205 Å for MgH₂-β; a =b= 4.5172 Å and c = 2.943 Å for TiO₂-rutile)[36], which can facilitate the formation of coherent MgH₂-TiO₂ interfaces between matrix and catalyst[38]. Another hypothesis for the difference

in catalytic performance between the titania polymorphs is related to the formation of reduced Ti^{+3} species (which was found to play an important role in catalytic mechanism for the hydrogen desorption process of magnesium hydride[39]), as TiO_2-rutile is more prompt to be reduced in hydrogen-containing atmosphere than anatase[37,38] (the reduction rate of rutile – per unit surface area – is 2.5 times faster than anatase's)[40].

4. Conclusions

The employment of the dark-field technique presented in this study was efficient in allowing the observation of TiO_2 nanoparticles within a MgH_2-TiO_2 composite (even at a small catalyst content of 5 wt% TiO_2).

The analyses of the pure additives indicated that NR550 and NR650 consisted of a mixture of nanorods and nanoparticles of TiO_2-anatase while NR750 was composed of coarser TiO_2-anatase nanoparticles with a small content of rutile. As a general trend, the increase in heat treatment temperature of titanate nanotubes led to the reduction in the fraction of nanorods and the increase in the average nanoparticles size.

XRD of the composites showed that there was not a noticeable difference in crystallographic composition among the composites, all of which were consisted of a mixture of MgH_2-β and MgH_2-γ with a small content of metallic magnesium.

The hydrogen sorption kinetics results showed that the addition of the nanomaterials to the magnesium hydride had a positive effect in the sorption kinetics for all the additives used in comparison to pure hydride.

The catalysts with the two best performances were NR750 and NR550, respectively, which were easily distinguishable during desorption test at 350 °C. The high difference in specific area between the two catalysts with the best performances suggests that the surface area was not of paramount importance to determine their kinetic behavior. It is suggested that the best performance of NR750 is due to the presence of a greater amount of TiO_2-rutile, which has been observed to present higher catalytic activity than TiO_2-anatase in MgH_2/Mg systems[36-38]. The reason for this is attributed to either the similarity in crystal structure and cell parameters[36] or the formation of Ti^{+3} species due to rutile presenting higher reduction rate than anatase in a hydrogen reducing atmosphere[37,38,40].

The effect of the nanomaterials' morphology was not conclusive. However, the better performance of NR550 compared to NR650 (which presented similar specific surface area and average particle size) might indicate a positive effect of the unidimensional morphology as the former one presented a higher fraction of nanorods.

6. References

1. Lynch FE. Metal hydride practical applications. *Journal of the Less Common Metals*. 1991;172-174(Pt 3):943-958.

2. Mueller WM. Hydrides in Nuclear Reactor Applications. In: Mueller WM, Blackledge JP, Libowitz GG, eds. *Metal Hydrides*. Chap 2. New York: Academic Press; 1968. p. 21-50.

3. Crabtree GW, Dresselhaus MS, Buchanan MV. The Hydrogen Economy. *Physics Today*. 2004;57(12):39-44.

4. Gandía LM, Arzamendi G, Diéguez PM. Renewable Hydrogen Energy: An Overview. In: Gandía LM, Arzamendi G, Diéguez PM, eds. *Renewable Hydrogen Technologies - Production, Purification, Storage, Applications and Safety*. Amsterdam: Elsevier; 2013. p. 1-17.

5. Biswas R. *Hydrogen Storage: Materials, Technologies and Global Markets*. Chapel Hill: BCC Publishing; 2017.

6. Jain IP, Lal C, Jain A. Hydrogen storage in Mg: A most promising material. *International Journal of Hydrogen Energy*. 2010;35(10):5133-5144. DOI: http://dx.doi.org/10.1016/j.ijhydene.2009.08.088

7. Korte C, Mandt T, Bergholz T. Physics of Hydrogen. In: Stolten D, Emonts B, eds. *Hydrogen Science and Engineering: Materials, Processes, Systems and Technology*. Weinheim: Wiley-VCH; 2016. DOI: http://doi.wiley.com/10.1002/9783527674268.ch24

8. Johansson E. *Synthesis and Characterisation of Potential Hydrogen Storage Materials*. [dissertation]. Uppsala: Uppsala University; 2004.

9. Barkhordarian G, Klassen T, Bormann R. Kinetic investigation of the effect of milling time on the hydrogen sorption reaction of magnesium catalyzed with different Nb_2O_5 contents. *Journal of Alloys and Compounds*. 2006;407(1-2):249-255. DOI: https://doi.org/10.1016/j.jallcom.2005.05.037

10. Schlapbach L, Shaltiel D, Oelhafen P. Catalytic effect in the hydrogenation of Mg and Mg compounds: surface analysis of Mg-Mg_2Ni and Mg_2Ni. *Materials Research Bulletin*. 1979;14(9):1235-1246. DOI: https://doi.org/10.1016/0025-5408(79)90220-4

11. de Abreu MAS, Morgado E Jr, Jardim PM, Marinkovic BA. The effect of anatase crystal morphology on the photocatalytic conversion of NO by TiO_2-based nanomaterials. *Central European Journal of Chemistry*. 2012;10(4):1183-1198. DOI: https://doi.org/10.2478/s11532-012-0040-3

12. Harzer GS, Orfanidi A, El-Sayed H, Madkikar P, Gasteiger HA. Tailoring Catalyst Morphology towards High Performance for Low Pt Loaded PEMFC Cathodes. *Journal of the Electrochemical Society*. 2018;165(10):F770-F779. DOI: 10.1149/2.0311810jes

13. Taylor MG, Austin N, Gounaris CE, Mpourmpakis G. Catalyst Design Based on Morphology- and Environment-Dependent Adsorption on Metal Nanoparticles. *ACS Catalysis*. 2015;5(11):6296-6301. DOI: https://doi/10.1021/acscatal.5b01696

14. Malik R, Kumar A, Nehra SP, Rana PS. Morphology dependent catalytic activity of TiO₂ nanostructures towards photodegradation of Rose Bengal. *AIP Conference Proceedings*. 2015;1675(1):020039. DOI: https://doi.org/10.1063/1.4929197

15. Nguyen-Phan TD, Shin EW. Morphological effect of TiO₂ catalysts on photocatalytic degradation of methylene blue. *Journal of Industrial and Engineering Chemistry*. 2011;17(3):397-400. DOI: https://doi.org/10.1016/j.jiec.2011.05.013

16. Xie X, Li Y, Liu ZQ, Haruta M, Shen W. Low-temperature oxidation of CO catalysed by Co₃O₄ nanorods. *Nature*. 2009;458(7239):746-749. DOI: 10.1038/nature07877

17. Brum MC, da Conceição MOT, Jardim PM, dos Santos DS. The use of one-dimensional Niobate to improve MgH₂ hydrogen sorption. *Journal of Alloys and Compounds*. 2014;615(Suppl 1):S698-S701. DOI: https://dx.doi.org/10.1016/j.jallcom.2013.12.148

18. Ismail M, Juahir N, Mustafa NS. Improved Hydrogen Storage Properties of MgH₂ Co-Doped with FeCl₃ and Carbon Nanotubes. *The Journal of Physical Chemistry C*. 2014;118(33):18878-18883. DOI: http://pubs.acs.org/doi/10.1021/jp5046436

19. Campos RBV, Camargo Junior SAS, Brum MC, dos Santos DS. Hydrogen Uptake Enhancement by the Use of a Magnesium Hydride and Carbon Nanotubes Mixture. *Materials Research*. 2017 Nov 27;20(Suppl 1):85-88. DOI: http://dx.doi.org/10.1590/1980-5373-mr-2017-0445

20. Jardim PM, da Conceição MOT, Brum MC, dos Santos DS. Hydrogen sorption kinetics of ball-milled MgH₂-TTNT nanotubes with different sodium contents. *Journal of Alloys and Compounds*. 2014;615(Suppl 1):S711-S714. DOI: http://dx.doi.org/10.1016/j.jallcom.2014.01.244

21. Jardim PM, da Conceição MOT, Brum MC, dos Santos DS. Hydrogen sorption kinetics of ball-milled MgH₂-TiO₂ based 1D nanomaterials with different morphologies. *International Journal of Hydrogen Energy*. 2015;40(47):17110-17117. DOI: https://doi.org/10.1016/j.ijhydene.2015.06.172

22. Kasuga T, Hiramatsu M, Hoson A, Sekino T, Niihara K. Titania Nanotubes Prepared by Chemical Processing. *Advanced Materials*. 1999;11(15):1307-1311. DOI: https://doi.org/10.1002/(SICI)1521-4095(199910)11:15<1307::AID-ADMA1307>3.0.CO;2-H

23. Morgado E Jr, de Abreu MAS, Pravia ORCC, Marinkovic BA, Jardim PM, Rizzo FC, et al. A study on the structure and thermal stability of titanate nanotubes as a function of sodium content. *Solid State Sciences*. 2006;8(8):888-900. DOI: https://doi.org/10.1016/j.solidstatesciences.2006.02.039

24. Williams DB, Carter CB. The Instrument. In: Williams DB, Carter CB. *Transmission Electron Microscopy*. Boston, MA: Springer US; 2009. p. 141-171. DOI: https://doi.org/10.1007/978-0-387-76501-3_9

25. Yao B, Heinrich H, Smith C, van den Bergh M, Cho K, Sohn Y. Hollow-cone dark-field transmission electron microscopy for dislocation density characterization of trimodal Al composites. *Micron*. 2011;42(1):29-35. DOI: https://doi.org/10.1016/j.micron.2010.08.010

26. Schindelin J, Arganda-Carreras I, Frise E, Kaynig V, Longair M, Pietzsch T, et al. Fiji: an open-source platform for biological-image analysis. *Nature Methods*. 2012;9(7):676-682. DOI: 10.1038/nmeth.2019

27. Buades A, Coll B, Morel JM. Non-Local Means Denoising. *Image Processing On Line*. 2011;1:208-212. DOI: https://doi.org/10.5201/ipol.2011.bcm_nlm

28. Moriwaki T, Akahama Y, Kawamura H, Nakano S, Takemura K. Structural Phase Transition of Rutile-Type MgH₂ at High Pressures. *Journal of the Physical Society of Japan*. 2006;75(7):074603. DOI: https://doi.org/10.1143/JPSJ.75.074603

29. Danaie M, Tao SX, Kalisvaart P, Mitlin D. Analysis of deformation twins and the partially dehydrogenated microstructure in nanocrystalline magnesium hydride (MgH₂) powder. *Acta Materialia*. 2010;58(8):3162-3172. DOI: https://doi.org/10.1016/j.actamat.2010.01.055

30. Danaie M, Mitlin D. TEM analysis and sorption properties of high-energy milled MgH₂ powders. *Journal of Alloys and Compounds*. 2009;476(1-2):590-598. DOI: https://doi.org/10.1016/j.jallcom.2008.09.078

31. Mirabile Gattia D, Di Girolamo G, Montone A. Microstructure and kinetics evolution in MgH₂–TiO₂ pellets after hydrogen cycling. *Journal of Alloys and Compounds*. 2014;615(Suppl 1):S689-S692. DOI: https://doi.org/10.1016/j.jallcom.2013.12.003

32. Croston DL, Grant DM, Walker GS. The catalytic effect of titanium oxide based additives on the dehydrogenation and hydrogenation of milled MgH₂. *Journal of Alloys and Compounds*. 2010;492(1-2):251-258. DOI: https://doi.org/10.1016/j.jallcom.2009.10.199

33. Pukazhselvan D, Nasani N, Correia P, Carbó-Argibay E, Otero-Irurueta G, Stroppa DG, et al. Evolution of reduced Ti containing phase(s) in MgH₂/TiO₂ system and its effect on the hydrogen storage behavior of MgH₂. *Journal of Power Sources*. 2017;362:174-183. DOI: https://doi.org/10.1016/j.jpowsour.2017.07.032

34. Pukazhselvan D, Nasani N, Sandhya KS, Singh B, Bdikin I, Koga N, et al. Role of chemical interaction between MgH₂ and TiO₂ additive on the hydrogen storage behavior of MgH₂. *Applied Surface Science*. 2017;420:740-745. DOI: https://doi.org/10.1016/j.apsusc.2017.05.182

35. Zhang X, Leng Z, Gao M, Hu J, Du F, Yao J, et al. Enhanced hydrogen storage properties of MgH₂ catalyzed with carbon-supported nanocrystalline TiO₂. *Journal of Power Sources*. 2018;398:183-192. DOI: https://doi.org/10.1016/j.jpowsour.2018.07.072

36. Jung KS, Kim DH, Lee EY, Lee KS. Hydrogen sorption of magnesium hydride doped with nano-sized TiO₂. *Catalysis Today*. 2007;120(3-4):270-275. DOI: https://doi.org/10.1016/j.cattod.2006.09.028

37. Pandey SK, Bhatnagar A, Shahi RR, Hudson MSL, Singh MK, Srivastava ON. Effect of TiO$_2$ Nanoparticles on the Hydrogen Sorption Characteristics of Magnesium Hydride. *Journal of Nanoscience and Nanotechnology*. 2013;13(8):5493-5499. DOI: https://doi.org/10.1166/jnn.2013.7516

38. Vujasin R, Mraković A, Kurko S, Novaković N, Matović L, Novaković JG, et al. Catalytic activity of titania polymorphs towards desorption reaction of MgH$_2$. *International Journal of Hydrogen Energy*. 2016;41(8):4703-4711. DOI: https://doi.org/10.1016/j.ijhydene.2016.01.095

39. Cui J, Wang H, Liu J, Ouyang L, Zhang Q, Sun D, et al. Remarkable enhancement in dehydrogenation of MgH$_2$ by a nano-coating of multi-valence Ti-based catalysts. *Journal of Materials Chemistry A*. 2013;1(18):5603-5611. DOI: 10.1039/C3TA01332D

40. Rekoske JE, Barteau MA. Isothermal Reduction Kinetics of Titanium Dioxide-Based Materials. *The Journal of Physical Chemistry B*. 1997;101(7):1113-1124. DOI: http://dx.doi.org/10.1021/jp9620025